

Closed-Form Analytical Investigation of Space-Vector PWM Inverter Fed Induction Motor Drive under DC-Bus Voltage Pulsation

JIRI KLIMA

Department of Electrical Engineering and Automation
 Technical Faculty of CZU in Prague
 CZECH REPUBLIC
klima@tf.czu.cz

Abstract—Voltage sag or unbalance conditions at the input rectifier stage of the ac-dc-ac rectifier-inverter induction motor drive can cause the significant amounts of harmonic voltage at twice the line frequency $2f_1$. This voltage ripple can have a degrading effect on the induction-machine performance characteristics. This paper presents an analytical closed-form mathematical model and analysis of the impact of DC-bus ripple voltage of the three-phase voltage source inverter (VSI) with the space-vector PWM (SVPWM) on the induction machine phase voltages, currents and torque pulsations. The analytical expressions for the voltage and current space-vectors as a function of the DC-bus voltage pulsation are derived. From the current space vectors the torque behavior is estimated, again as a function of DC-link voltage pulsation. Next, it is shown, that DC-link voltage ripple components may cause large torque pulsation. The proposed analytical method is based on the mixed p-z approach [13], enabling presentation of the results in lucid and closed-form. To verify the effectiveness of the proposed analytical model, experimental results based on laboratory setup were performed.

Key-Words—PWM inverter, mathematical model, induction motor, torque pulsation.

1 Introduction

In most of the industrial applications the induction machine is supplied by a voltage source inverter (VSI). The inverter experiences in some situations a substantial ripple of the dc bus voltage that may negatively affect the supply of the connected electric drives. Input voltage unbalance and sag conditions can have serious performance consequences in induction motors.

An increase in electric losses, excessive rise of the motor temperature, appearance of the torque pulsation, and noise problems are just some of the possible problems [1].

So, the analysis of the dc link pulsation and its influence on the motor performances is of great importance.

The dc bus voltage pulsation is composed of several sources such as follows [1], [2], [5]:

- a) The diode rectification of the AC line voltage causes pulsation components
- b) Unbalance in the AC power supply generates 100 or 120-Hz component
- c) In some faulty conditions in the front-end rectifier DC-link voltage may consist again pulsation
- d) Transient voltage sags in the three-phase input line voltages can cause the rectifier stage to transition into single-phase rectifier operation with corresponding dc bus voltage pulsation.

All these conditions create significant amount of voltage harmonics on the dc link at twice the line frequency. This dc link voltage ripple at the inverter input terminal will affect the PWM output voltage waveforms, causing harmonic distortion currents to flow in machine.

The mathematical model providing closed-form expressions to estimate the machine currents and torque waveforms as a consequence of dc link voltage ripple was presented in [3]. It was derived that the dominant as frequency component that appears in the dc link voltage during single-phase operation mode falls at twice the excitation angular frequency.

$(2\omega_1)$, and as a result, (equation (6) in [3]), the dc bus voltage can be approximated by the constant value V_{dc} and the pulsation part

$$V_{dc2} \cos(2\omega_1 t + \theta_2) ..,$$

where V_{dc2} is the amplitude of the second-harmonic voltage component, and θ_2 is the corresponding phase angle.

The paper [3] has analyzed the performance effects of voltage sag and imbalance conditions on the dc-link the output inverter and following negative effect on the induction machine performance characteristics. But in this paper the analyses is very simplified by the assumption that the inverter PWM voltage was approximated only by the fundamental harmonic

which is far from reality especially in low and medium switching frequency.

This paper presents a mathematical model which enables us to solve both the steady-state and transient-state performance of the three-phase VSI with the SVM feeding induction motor under dc link voltage ripple. The solution makes use of the Laplace and modified Z-transforms of the space vectors (mixed p-z approach [13], [14]). From the Laplace transform of the stator voltage vectors we can also derive Fourier series to predict the voltage harmonic spectra.

Analysis is made on the assumption that the motor runs at a constant speed. The electromechanical time constant is much larger than the electrical ones and therefore it is reasonable to assume that the rotor speed remains constant during a sampling period

The attention is focused on the calculation of the closed-form expressions for the stator and rotor currents. From these equations an analytical expression for the electromagnetic torque in dependence of the dc link pulsation is derived. Torque ripple deteriorates the static and dynamic characteristics of induction motors and it may become an important issue in induction motor design. It may cause mechanical oscillations, which are particularly dangerous in resonant frequencies of the load. Moreover, torque ripple leads to increase of the motor noise and to derating. Particularly the appearance of the sixth torque harmonic was observed by many researchers [5] [6]. But in this paper it will be shown that dc link ripple voltage components may arise an additional large torque ripple component.

The paper contributes to a better understanding of the effects of dc link voltage ripple conditions on the operation of induction machine by providing closed-form expressions both in time and frequency domain. In particular, this mathematical model provides a useful tool for the development of the dc link ripple mitigation technique by a proper modulation technique of the inverter.

The proposed mathematical model has also been verified by experiment. Experimental results show good agreement with theoretical prediction.

2 Stator Voltage Space-Vectors

A simplified scheme of the system is shown in Fig.1. The input part (solid lines) consists of the front-end PWM rectifier that is connected to the supply through input inductors L . The three-phase input line-inductances (L) are balanced. The dc bus voltage is buffered by two dc bus capacitances C_{dc} . The output part (dotted lines) is composed of the PWM inverter consisting of six IGBT switches and their antiparallel

diodes. The PWM voltage waveforms are delivered to the induction machine following a constant volts-per-hertz algorithm.

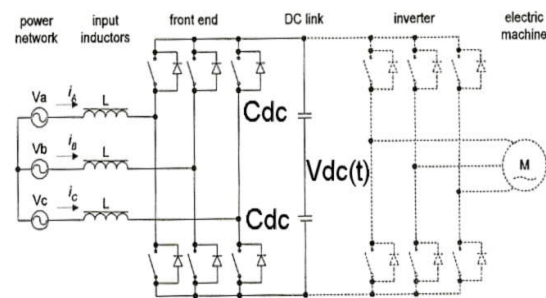


Fig.1. Diagram of investigated system

This paper is focused primarily with the output part of the drive. (VSI feeding induction motor drive-dotted lines). This approach takes into account the dc link voltage ripple, due to the finite dc link capacitors. We assume that dc link voltage contains both the constant and pulsation parts that may be expressed as:

$$V_{dc}(t) = V_{dc0} + \sum_{i=1}^{\infty} \Delta V_{dci} \cos(i2\omega_1 t + \psi_i) \quad (1a)$$

The voltage ripple appearing across the dc link capacitor terminals contains, only even order harmonics [3].

The dominant ac frequency component that appears in the dc link voltage falls at twice the excitation frequency ($2f_1$).

As a result for the closed-form mathematical solution, we suppose as in [3], that the dc link voltage can be approximated by the constant average value V_{dc} and pulsation part $\Delta V_{dc} \cos 2\omega_1 t$, where

ω_1 is an angular frequency of the supply voltage ($2\pi 50$ or $2\pi 60$, s⁻¹).

But if needed we can take into consideration also the next higher harmonics with the angular frequency $4\omega_1$.

The switching elements will be considered as ideal switches. We also assume constant rotor speed and linear parameters of the motor.

As the dominant ac component in the resulting dc bus voltage $V_{dc}(t)$ is created by the second-harmonic voltage component it also dominates in generation of undesirable effects in the induction-machine operating performance characteristics. Attention is focused next on developing the closed-form mathematical model that quantifies the induction-machine performance effects caused by this second-harmonic voltage component.

The stator voltage space vector can be expressed in the complex $\alpha\beta$ plane with respect to $\pi/3$ symmetry as follows:

$$V(n, \varepsilon) = (V_{dc} + \Delta V_{dc}) \cos(2\omega_1(n + \varepsilon)T) \frac{2}{3} e^{j\omega_0 T n} \quad (1b)$$

where

$$\omega_0 = \frac{2\pi}{T_0} \text{ is the inverter output fundamental angular frequency.}$$

In (1b) time is expressed in per units as

$$t = (n + \varepsilon)T = (n + \varepsilon) \frac{T_0}{6} \quad (2)$$

where $T = T_0/6$ is a sector period, n is number of a sector and ε is a per unit time inside of a sector T .

$$0 \leq \varepsilon \leq 1 \quad (2a)$$

To express the voltage space vector with SVPWM we must include in (1b) also the modulation function and the stator voltage vector is calculated as follows:

$$V(n, \varepsilon) = \frac{[V_{dc} + \Delta V_{dc} \cos 2\omega_1(n + \varepsilon)T]}{3} \quad (3)$$

$$2e^{jn\frac{\pi}{3}} \sum_k f(\varepsilon, k) e^{j\pi\frac{\alpha_k}{3}} = V_d(n, \varepsilon) + V_p(n, \varepsilon)$$

In (3) $V_d(n, \varepsilon)$ is the voltage space vector created from the constant part of the dc bus voltage (V_{dc}), and $V_p(n, \varepsilon)$ is the voltage space vector caused from the second-harmonic voltage component (ΔV_{dc}).

And

$$\sum_k f(\varepsilon, k) e^{j\pi\frac{\alpha_k}{3}}$$

is the modulation function given by the switching instants within k -the pulse. This function contains both time and phase vector dependency.

Time dependency is given as follows:

$$f(\varepsilon, k) = 1, \text{ for } \dots \varepsilon_{kA} \leq \varepsilon \leq \varepsilon_{kB} \quad , \quad f(\varepsilon, k) = 0 \text{ else} \quad (3a)$$

where: ε_{kA} is start point setting per unit time of k -the pulse

ε_{kB} is end point setting per unit time of k -the pulse

the duty ratio switching time is :

$$\Delta\varepsilon_k = \varepsilon_{kB} - \varepsilon_{kA} \quad (3b)$$

The expressions for the switching times are given in [6].

Phase dependency is given by the function

$$g(k) = e^{j\frac{\pi}{3}\alpha_k} \quad (3c)$$

Where α_k shows which voltage vector is used in k -the pulse .

For the conventional space-vector PWM (CSVPWM) where two adjacent space vectors within a sampling period are used, α_k can be 0 or 1(i.e. voltage vectors in n -the sector period can have direction

$$e^{j\frac{\pi}{3}n} e^{j\frac{\pi}{3}0} = e^{j\frac{\pi}{3}n}, \text{ and } e^{j\frac{\pi}{3}n} e^{j\frac{\pi}{3}1} = e^{j\frac{\pi}{3}(n+1)}.$$

In the first sector during the first two sampling periods the following voltage vector sequence is used:

$$(V_0-V_1-V_2-V_0), \quad (V_0-V_2-V_1-V_0)$$

We can define α_k as follows:

$$\alpha_{2m-1} = \frac{1+(1)^m}{2}, \alpha_{2m} = \frac{1+(1)^{m+1}}{2} \quad (3d)$$

m is a number of sampling periods

The trajectory of $V(n, \varepsilon)$ in the complex $\alpha\beta$ plane for $\Delta V_{dc} = 0.05$,and $f_0=f_1=50\text{Hz}$, $f_{sw}=3000 \text{ Hz}$ is shown in Fig.2

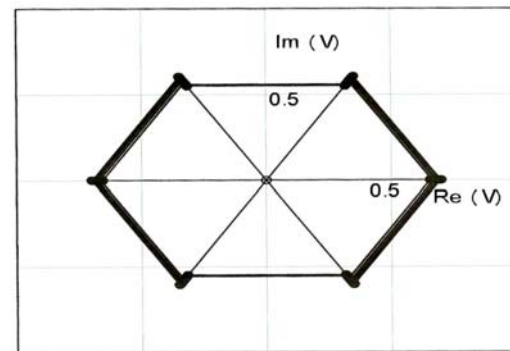


Fig.2 Voltage space vector trajectory with dc-link pulsation component $\Delta V_{dc} = 0.05$

Using well known formula for cosine function

$$\cos x = \frac{e^{jx} + e^{-jx}}{2} \quad (4)$$

we can write for the pulsating part in (3)

$$V_p(n, \varepsilon) = \frac{\Delta V_{dc}}{3} e^{j2\omega_1 T(n+\varepsilon)} e^{jn\frac{\pi}{3}} \sum_k f(\varepsilon, k) e^{j\pi\frac{\alpha_k}{3}} + \frac{\Delta V_{dc}}{3} e^{-j2\omega_1 T(n+\varepsilon)} e^{jn\frac{\pi}{3}} \sum_k f(\varepsilon, k) e^{j\pi\frac{\alpha_k}{3}} = V_{pp}(n, \varepsilon) + V_{pn}(n, \varepsilon) \quad (5)$$

From (5) it may be seen that pulsation part of the voltage space vector $V_p(n, \varepsilon)$ may be resolved into two components: positive $V_{pp}(n, \varepsilon)$ and negative $V_{pn}(n, \varepsilon)$

The trajectories of the both parts in the complex plane for the same operating conditions used to calculate waveform in Fig.2, are shown in Fig.3

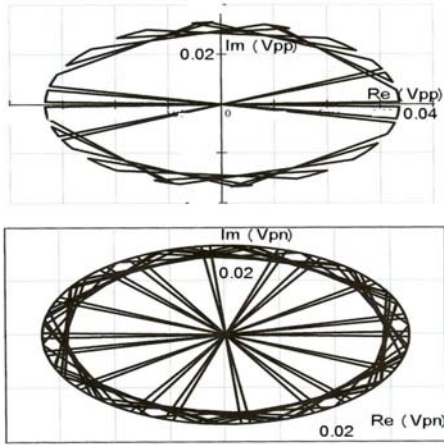


Fig. 3 Trajectories of two parts creating voltage space vector with DC-link pulsation component $\Delta V_{dc}=0.05$

3 Closed-Form Mathematical

3.1. Induction-Machine Circuit Analysis

Using the mixed p-z approach as shown in [13], [14] we can derive the closed-form analytical expressions for the stator and/or rotor currents and also for the electromagnetic torque.

From these relations we can estimate the influence of the dc link voltage pulsation on the currents and electromagnetic torque waveforms.

First, we can derive the Laplace transform of the symmetrical voltage vector sequences (3). For that we can use the relation between the Laplace and modified Z transforms [12].

Using (2) and its derivation $dt=Td\varepsilon$ we can derive the Laplace transforms of the periodic waveform as:

$$V(p) = \sum_{n=0}^{\infty} \left(\int_0^1 V(n, \varepsilon) e^{-p(n+\varepsilon)T} T d\varepsilon \right) = T \int_0^1 V(z, \varepsilon) e^{-pT\varepsilon} d\varepsilon \quad (6)$$

where:

$$z=epT, \quad (7)$$

and $V(z, \varepsilon)$ is the modified Z transform of $V(n, \varepsilon)$. Substituting (3) into (6) with the help of the Z transform of exponential functions we can find the Laplace transform of the stator voltage vector as follows:

$$V_1(p) = \frac{2}{3} V_{dc} \frac{1}{p} \frac{e^{pT}}{e^{pT} - e^{j\frac{\pi}{3}}} \sum_k (e^{-pT\varepsilon_{kA}} - e^{-pT\varepsilon_{kB}}) + \frac{1}{3} \Delta V_{dc} \frac{1}{p-2j\omega_1} \frac{e^{pT}}{e^{pT} - e^{j(\frac{\pi}{3}+2\omega_1 T)}} \sum_k (e^{-T\varepsilon_{kA}(p-2j\omega_1)} - e^{-T\varepsilon_{kB}(p-2j\omega_1)}) + \frac{1}{3} \Delta V_{dc} \frac{1}{p+2j\omega_1} \frac{e^{pT}}{e^{pT} - e^{j(\frac{\pi}{3}-2\omega_1 T)}} \sum_k (e^{-T\varepsilon_{kA}(p+2j\omega_1)} - e^{-T\varepsilon_{kB}(p+2j\omega_1)}) = V_0(p) + V_{1P}(p-2j\omega_1) + V_{1N}(p+2j\omega_1) \quad (8)$$

Equation (8) is the Laplace transform of the stator voltage vector, respecting the influence of the dc-link voltage ripple. It contains three parts. The first term is the Laplace transform of the stator voltage vector with constant value in the dc link voltage. The last two terms are the Laplace transform of the positive and the negative ripple components of the dc link voltage.

When we know the Laplace transform of the stator voltage vectors we can derive the Laplace transform of the motor current vectors.

In order to calculate the motor current space vectors, it is convenient to carry out the analysis in the stator reference frame.

The Laplace transform of the stator and the rotor currents may be expressed as follows:

$$I_S(p) = V_1(p) \frac{A_S(p)}{B_S(p)} = V_1(p) \frac{k_R + p - j\omega}{\sigma L_S (p-p_1)(p-p_2)} \quad (9)$$

$$I_R(p) = V_1(p) \frac{A_R(p)}{B_R(p)} = -V_1(p) \frac{L_m (p-j\omega)}{\sigma L_S L_R (p-p_1)(p-p_2)}$$

In the foregoing equations, R_S is the stator resistance, R_R the rotor resistance, L_S the stator self-inductance,

L_R the rotor self-inductance, L_m is the mutual inductance, and ω the rotor electrical angular velocity

$$\sigma=1-L_m/(L_S L_R), k_S=R_S/L_S, k_R=R_R/L_R,$$

The roots of the characteristic equation are given as follows:

$$p_{1,2} = \frac{-(k_S + k_R - j\sigma\omega)}{2\sigma} \pm \sqrt{\left(\frac{k_S + k_R - j\sigma\omega}{2\sigma}\right)^2 + \frac{j\omega k_S - k_S k_R}{\sigma}} \quad (10)$$

The inverse Laplace transform of (9) cannot be solved directly using the residue theorem, as (9) contains infinite numbers of poles given by the following equations:

$$e^{j\frac{\pi}{3}} - e^{pT} = 0$$

$$e^{j(\frac{\pi}{3}-2\omega_1 T)} - e^{pT} = 0, e^{j(\frac{\pi}{3}+2\omega_1 T)} - e^{pT} = 0 \quad (11)$$

The solution of the time dependency of the motor current vectors can be found in the closed form as presented in [15].

If we use the Heaviside theorem

$$L^{-1} \left\{ \frac{A(p)}{pB(p)} \right\} = \frac{A(0)}{B(0)} + \sum_k \frac{A(p_k)}{p_k B'(p_k)} e^{p_k T} \quad (12)$$

and also the formula for multiplication by an exponential function

$$L \left\{ e^{j\omega T} f(t) \right\} = F(p - j\omega T) \quad (13)$$

where $B'(p_k) = (dB/dp)p=p_k$ and symbols $L\{\}$ and $L^{-1}\{\}$ mean the direct and inverse Laplace transforms, respectively, we can transform the motor currents (9) into the modified Z-domain [13]. After doing that, we can use the residue theorem in the modified Z-transform to find the analytical closed-form solution both for the stator and for the rotor current vectors. Details of this analysis and the corresponding coefficients are provided in the Appendix and in [14]. The solution contains both the steady-state and transient components. As our attention is focused on the steady-state solution, applying superposition, the stator and rotor currents will have the closed-form solution shown in (14), for $n \rightarrow \infty$,

$$I_{yS}(n, \varepsilon) = I_{yS}^1(0)e^{j\frac{\pi}{3}(n+1)} + I_{yS}^1(p_s)e^{j\frac{\pi}{3}(n+1)} e^{p_s T \varepsilon} +$$

$$I_{yS}^2(2j\omega_1)e^{j\frac{\pi}{3}(n+1)} e^{2j\omega_1 T(n+\varepsilon)} + I_{yS}^2(p_s - 2j\omega_1)e^{j(\frac{\pi}{3}+2j\omega_1 T)(n+1)} e^{p_s T \varepsilon} +$$

$$I_{yS}^2(-2j\omega_1)e^{j\frac{\pi}{3}(n+1)} e^{-2j\omega_1 T(n+\varepsilon)} + I_{yS}^2(p_s + 2j\omega_1)e^{j(\frac{\pi}{3}-2j\omega_1 T)(n+1)} e^{p_s T \varepsilon} =$$

$$I_{y0}(n, \varepsilon) + I_{yp}(n, \varepsilon) + I_{yn}(n, \varepsilon) \quad (14)$$

where the subscript y stands for the stator (y=S) and the rotor (y=R) variables. Similarly to (8) the overall steady-state stator/rotor currents contain three parts (terms from constant, positive and negative bus voltages, respectively).

These components are shown in Fig.4a and 4b. From Fig.4a we can see the space-vector current trajectories with and without respecting dec-link voltage ripple. The dc-link voltage ripple influence may be seen from Fig.4b. The upper plot of Fig.4b shows current space-vector trajectory from constant dc bus voltage, the middle and bottom plots show current space-vector trajectories from the positive and negative dc bus voltage components, respectively. Fig.5 shows the induction machine stator phase currents. Owing to the dc bus voltage pulsation the phase currents are highly distorted.

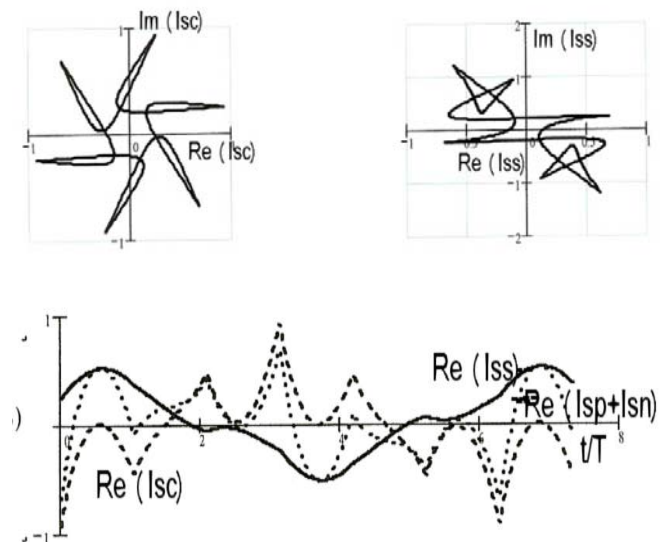


Fig.4a Closed-form analysis results of machine stator current vectors. $\Delta V_{dc} = 0.05$ -Six-Step waveforms

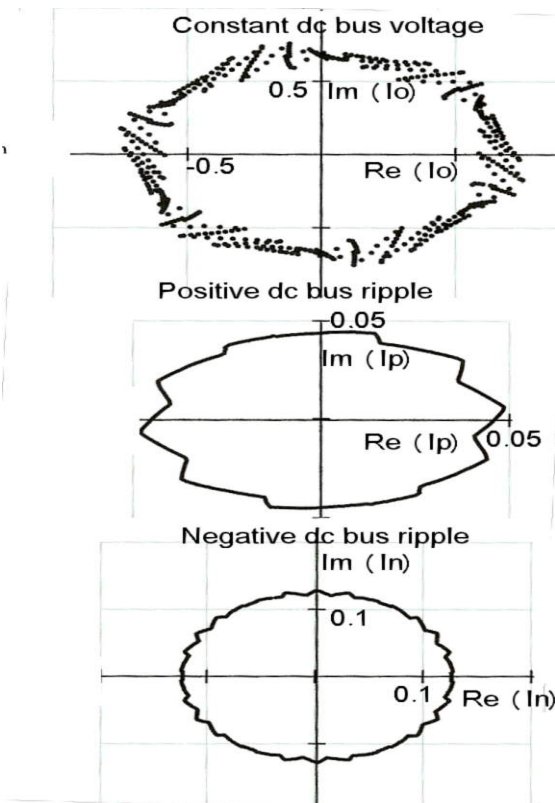


Fig.4b Closed-form analysis results of machine stator current vectors. $\Delta V_{dc}=0.05$, Space-Vector modulation

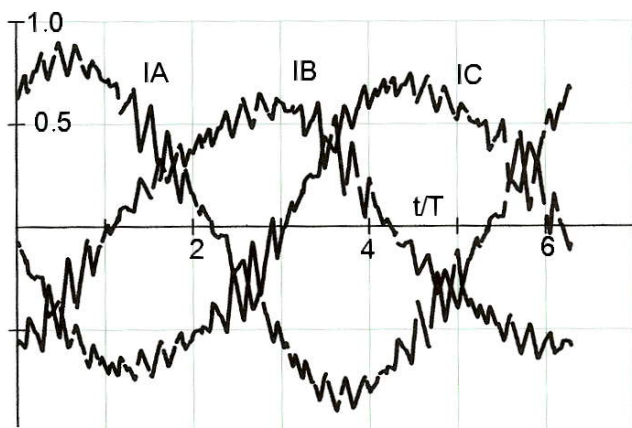


Fig.5 Closed-form analysis results of machine phase currents, $\Delta V_{dc}=0.05$,

3.2 Electromagnetic Torque

Torque ripple with low frequency may become an important issue in induction motor drives .It cause mechanical oscillations, which are particularly dangerous in resonance frequencies of the system [5].

This torque ripple is usually superimposed to the torque ripple of switching frequency. Since the switching frequency has usually high value, its effect will be suppressed by the electrical and mechanical damping of the motor and of the gear.

In steady state, along with an expected torque ripple of switching frequency, a superimposed pulsation was observed. Particularly, the appearance of the sixth torque harmonic was observed by many researchers [6], [8].

As it was shown in [8] the occurrence of zero vector intervals in PWM influences torque ripple, and leads to a sixth-order torque harmonics. But as it will be shown in the following part of this paper, dc bus voltage pulsation with angular frequency $2\omega_1$ may cause large torque pulsation with the same angular frequency.

The electromagnetic torque is given from the stator and rotor vector current by the following formula:

$$T_i(n, \varepsilon) = \frac{3}{2} L_m \frac{P}{2} \text{Re} \{ j I_s^*(n, \varepsilon) I_r(n, \varepsilon) \} \quad (15)$$

where symbol * means complex conjugate value and P is the number of poles.

The expression for the complex stator and rotor currents in (14) can be used to develop an expression for the product in (15) as follows:

$$\begin{aligned} T_i(n, \varepsilon) &= \frac{3}{2} L_m \frac{P}{2} \text{Re} \{ j I_{S0}^*(n, \varepsilon) I_{R0}(n, \varepsilon) \} + \\ &\frac{3}{2} L_m \frac{P}{2} \text{Re} \{ j (I_{Sp}^*(n, \varepsilon) + I_{Sn}^*(n, \varepsilon)) I_{R0}(n, \varepsilon) \} + \\ &\frac{3}{2} L_m \frac{P}{2} \text{Re} \{ j I_{S0}^*(n, \varepsilon) (I_{Rp}(n, \varepsilon) + I_{Rn}(n, \varepsilon)) \} + \\ &+ \frac{3}{2} L_m \frac{P}{2} \text{Re} \{ j (I_{Sp}^*(n, \varepsilon) + I_{Sn}^*(n, \varepsilon)) (I_{Rp}(n, \varepsilon) + I_{Rn}(n, \varepsilon)) \} \\ &= T_{i0}(n, \varepsilon) + T_{i1}(n, \varepsilon) + T_{i2}(n, \varepsilon) + T_{iC}(n, \varepsilon) \end{aligned} \quad (16)$$

This expression shows that, under unbalance input voltage conditions, the electromagnetic torque contains the following terms:

$T_{i0}(n, \varepsilon)$ is the electromagnetic torque without dc bus ripple component. It contains an average dc term and sixth-harmonic pulsations caused by the inverter switching frequency.

$T_{i1}(n, \varepsilon)$ and $T_{i2}(n, \varepsilon)$ represent the products of the complex conjugate stator currents from the constant/ripple dc bus and the complex rotor currents from the ripple/constant dc bus voltage.

$T_{iC}(n, \varepsilon)$ is the electromagnetic torque component from stator and rotor dc link pulsation parts. I has negligible value and we may put $T_{iC}(n, \varepsilon)=0$.

The separated torque components can be seen from Fig.6.

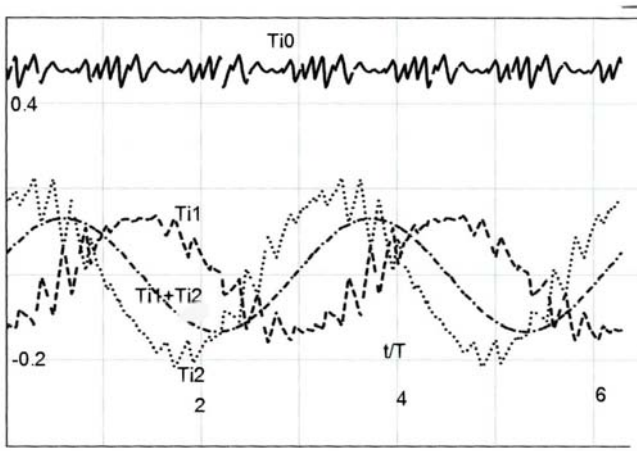


Fig.6 Closed-form analysis results of electromagnetic torque and its components. Solid line- overall pulsation torque ($T_{ipul}(n,\varepsilon)$), dashed line-first pulsation component ($T_{i1}(n,\varepsilon)$), dotted line-second pulsation component ($T_{i2}(n,\varepsilon)$). dash dotted line the overall pulsation component ($T_{i1}(n,\varepsilon)+ T_{i2}(n,\varepsilon)$), $f_0=f_1=50$ Hz, $f_{sw}=3000$ Hz, $\Delta U = 0.05$

The overall pulsating electromagnetic components and their sum given as follows:

$$T_{ipUL}(n,\varepsilon)= T_{i1}(n,\varepsilon)+ T_{i2}(n,\varepsilon)= A_T \cdot \sin(2 \cdot \omega_0 \cdot [(n+\varepsilon)T+\psi]) \quad (17)$$

Where A_T is an amplitude of the pulsating torque component (in Fig.6) we have $A_T=0.073$ p.u.) and ψ is a phase angle.

As can be seen from Fig.6 both electromagnetic components forming the pulsation part have opposite direction and their sum is the pulsating waveform with the sine time dependency (without any high frequency ripple). The frequency of the pulsation is given by the frequency of dc bus voltage pulsation $2\omega_1$.

3.3 Frequency Domain

We shall calculate the Fourier series of the periodic variation of the stator voltage space-vector

$$V(n, \varepsilon) = \sum_{k=-k_{max}}^{k_{max}} C_k e^{jk\omega_0 T(n+\varepsilon)} \quad (18)$$

Using superposition of the two parts of the dc bus voltage (constant and pulsation part) and (4), we can modify (18), as

$$V(n, \varepsilon) = \sum_{k=-k_{max}}^{k_{max}} C_k^1 e^{jk\omega_0 T(n+\varepsilon)} + \sum_{k=-k_{max}}^{k_{max}} C_k^2 e^{jk\omega_0 T(n+\varepsilon)} (e^{j2\omega_1 T(n+\varepsilon)} + e^{-2j\omega_1 T(n+\varepsilon)}) \quad (19)$$

To derive the coefficients of the Fourier analysis we can use the relation between the Laplace transform of the periodic waveform and Fourier coefficients:

$$C_\mu = \left[\frac{1}{T_1} (1 - \exp(-pT_0)) V(p) \right]_{p=j\mu\omega_0} \quad (20)$$

Substituting in. (20) from first part of (8) we get for the Fourier coefficients of the constant dc bus voltage :

$$C_\mu^1 = \frac{V_{dc}}{3} \frac{1}{\pi j \mu} \left[\frac{\exp(j\mu \frac{\pi}{3}) - \exp(-5j\mu \frac{\pi}{3})}{\exp(j\mu \frac{\pi}{3}) - \exp(j\frac{\pi}{3})} \right] \quad (21)$$

$$\sum_k \exp\left[\frac{j\pi\alpha_k}{3} \right] \left[\exp(-j1 \frac{\pi}{3} \varepsilon_{Ak}) - \exp(-j1 \frac{\pi}{3} \varepsilon_{Bk}) \right]$$

Equation (21) has non-zero value only for harmonics order:

$$\mu = 1 + 6v, \quad v = 0, \pm 1, \pm 2, \dots \quad (22)$$

By substituting (22) into (21) the Fourier coefficients are:

$$C_v^1 = \frac{2V_{dc}}{\pi j(1+6v)} \sum_k \exp\left[j\pi \frac{\alpha_k}{3} \right] \left[\exp(-j(1+6v) \frac{\pi}{3} \varepsilon_{Ak}) - \exp(-j(1+6v) \frac{\pi}{3} \varepsilon_{Bk}) \right] \quad (23)$$

Similarly, we can derive for the second part of (8)

$$C_v^2 = \frac{\Delta V_{dc}}{\pi j(1+6v)} \sum_k \exp\left[j\pi \frac{\alpha_k}{3} \right] \left[\exp(-j(1+6v) \frac{\pi}{3} \varepsilon_{Ak}) - \exp(-j(1+6v) \frac{\pi}{3} \varepsilon_{Bk}) \right] \quad (24)$$

$$= \frac{C_v^1}{V_{dc}} \frac{\Delta V_{dc}}{2}$$

The Fourier series expansion of the overall voltage space-vector will have the following form:

$$\begin{aligned}
 V(n, \varepsilon) = & \sum_{v=-v_{\max}}^{v_{\max}} C_v^1 e^{j(1+6v)\omega_0 T(n+\varepsilon)} + \\
 & \sum_{v=-v_{\max}}^{v_{\max}} C_v^1 \frac{\Delta V_{dc}}{2V_{dc}} e^{j(1+6v)\omega_0 T(n+\varepsilon)} e^{2j\omega_1(n+\varepsilon)T} + \quad (25) \\
 & \sum_{v=-v_{\max}}^{v_{\max}} C_v^1 \frac{\Delta V_{dc}}{2V_{dc}} e^{j(1+6v)\omega_0 T(n+\varepsilon)} e^{-2j\omega_1(n+\varepsilon)T}
 \end{aligned}$$

From (25) it may be seen that harmonic spectrum contains harmonics with frequencies $(1 + 6v)f_1$ and amplitudes C_v^1 as in VSI without dc bus pulsations and also harmonics with the sum and difference frequencies $(1 + 6v)f_1 + 2f_0$ and

$(1 + 6v)f_1 - 2f_0$, respectively, both with reduced

harmonic amplitudes $C_v^2 = C_v^1 \frac{\Delta V_{dc}}{2V_{dc}}$.

For example if $f_0 = f_1 = 50\text{Hz}$ we have harmonics $(1 + 6v)50\text{ Hz}$, $(1 + 6v)50 + 100\text{ Hz}$, $(1 + 6v)50 - 100\text{ Hz}$

It means that for $v = 0$ we get harmonics with frequencies 50,150 and -50 Hz

for $v = 1$ we get harmonics with frequencies 350,450 and 250 Hz

for $v = -1$ we get frequencies -250,-150 and -350 Hz , etc.

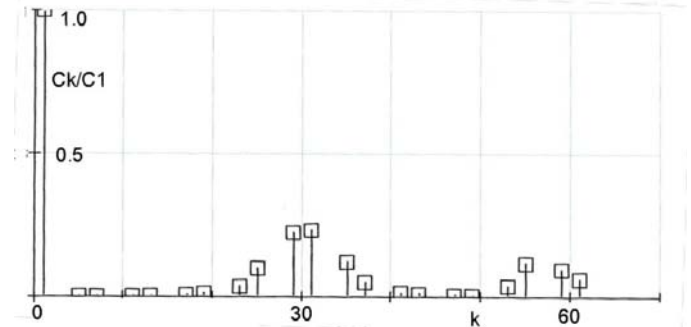
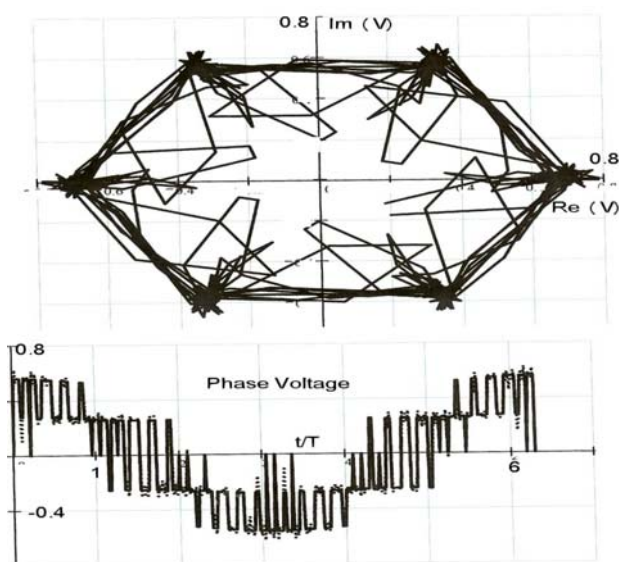


Fig.7 Fourier series expansion of the voltage space-vector (upper trace) and its phase-voltage waveform (bottom trace) $f_0 = f_1 = 50\text{Hz}$, $f_{sw}=3000\text{Hz}$, $\Delta V_{dc} = 0.05$, $k_{max}=30$

The Fourier series approximation of the voltage space-vectors trajectory is shown in upper plot of Fig.7. It is calculated from (23)-(25) for SVPWM, if we take into consideration $v_{\max} = 30$.

The phase voltage approximation can be calculated as a real part of (25) and is shown in middle plot of Fig.7 (dotted line). As can be seen by comparing with the theoretical voltage waveform (solid line) the correlation is high.

The harmonic spectrum $\frac{C_v^1}{C_{v=0}^1}$ given from (23) is

shown in bottom part of Fig.7 The harmonic spectrum is calculated for switching frequency 3000Hz and modulation index $m=1$. The harmonic spectrum is a typical for synchronous modulation. It means that ration of the switching and fundamental frequency is 60.

4 Experimental Results

Further, the analytical results and experimental waveforms for the sake of comparison are presented. All the analytical results were visualized from the derived equations by the program MATHCAD. Experimental tests have been carried out using 1.5-kW 400-V, 50-Hz induction machine mounted on a laboratory dc dynamometer.

The dc link voltage waveform is shown in Fig8. It is apparent from the Fig.8 that the dominant ac frequency component in the dc bus voltage under input voltage unbalance conditions appears at twice the input supply frequency ($2f_{14}$) providing confirmation of (1b).

First, the comparison is made for the case of square-waveforms (without modulation) as in that case we can see the most pronounced influence of the dc link voltage ripple. The current waveforms in Fig.9 for 5% dc link voltage ripple show the same features both for

the experiments and closed-form analytical results. The comparison is done for two values of slip. ($s=0.6$ and $s=0.026$), it means for two values of the load conditions, providing further confirmation of the closed-form analytical results.

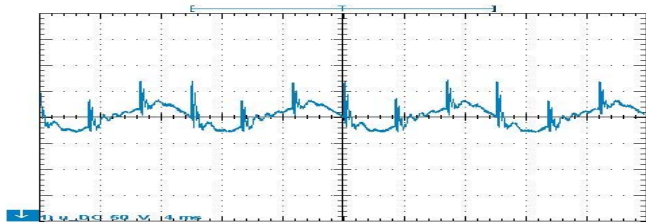
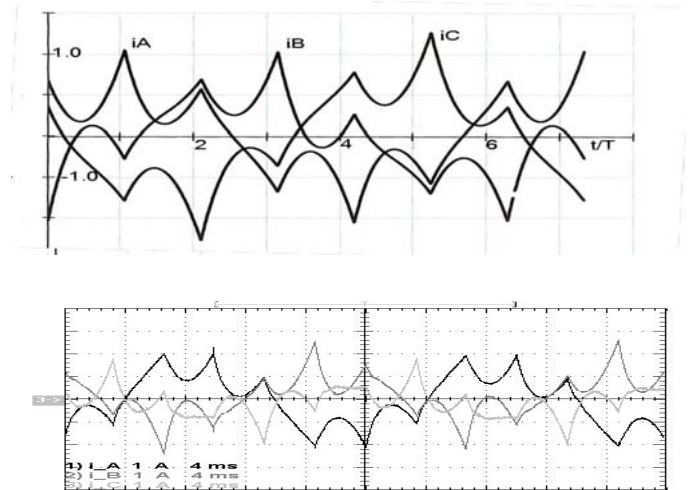
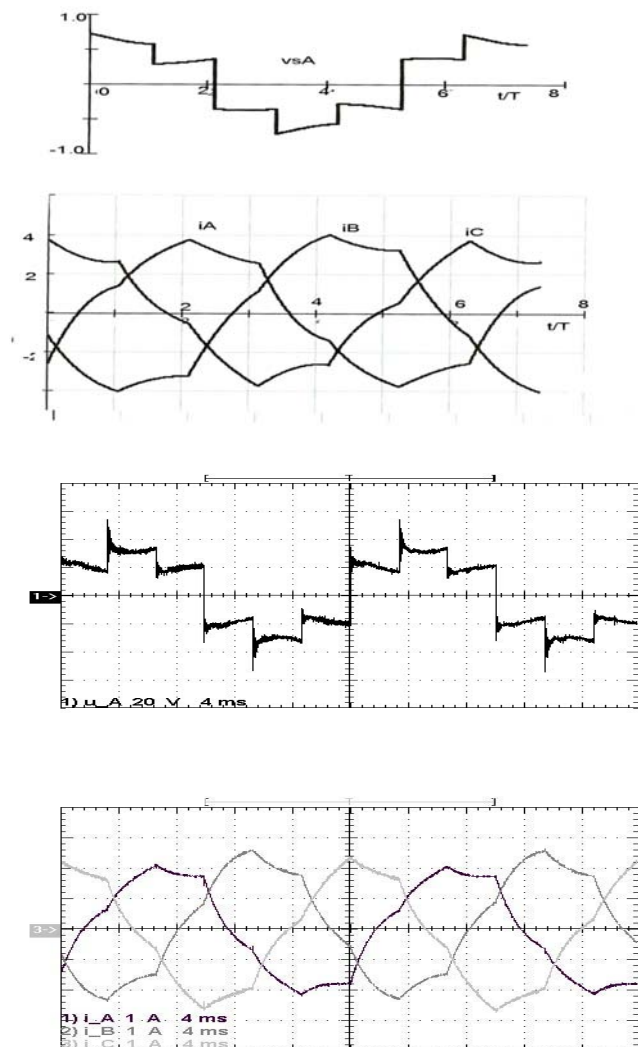


Fig.8 Rectified input line voltage with dc bus voltage ripple



b)

Fig.9 Closed-form analytical results and measured stator-current waveforms with dc bus voltage ripple $\Delta V_{dc} = 0.05$ a) for slip $s=0.6$, b) for slip $s=0.024$



a)

5 Conclusion

Analytical analysis and mathematical model of three-phase voltage source PWM inverter fed induction motor drive under DC-link ripple voltage component are presented in this paper. The analytical expressions for the voltage and current space-vectors as a function of the DC-link voltage pulsation are derived. By means of the modified Z-transform and the mixed p-z mathematical model we can estimate the separate parts of the solution to estimate the influence of the DC-link voltage pulsating on current and torque waveforms. Torque ripple produced in PWM inverter fed induction motor drives deteriorates both static and dynamic characteristics of drives. It was found that DC-link ripple voltage components with angular frequency ω_0 may cause large torque pulsation with the same angular frequency. This torque ripple may be even dangerous at resonance frequencies of the system.

6. Appendix

6.1 Closed-Form Derivation

Using (2) and (3) the Laplace transform of the load current can be expressed as:

$$\begin{aligned}
 I_y(p) &= V_1(p) \frac{A_y(p)}{B_y(p)} = \left\{ \frac{2}{3} V_{dc} \frac{1}{p} \frac{e^{pT}}{e^{pT} - e^{j\frac{\pi}{3}}} \right. \\
 &+ \sum_k (e^{-pT\epsilon_{kA}} - e^{-pT\epsilon_{kB}}) \frac{A_y(p)}{B_y(p)} + \\
 &\frac{1}{3} \Delta V_{dc} \frac{1}{p-2j\omega_1} \frac{e^{pT}}{e^{pT} - e^{j(\frac{\pi}{3}+2\omega_1 T)}} \\
 &+ \sum_k (e^{-T\epsilon_{kA}(p-2j\omega_0)} - e^{-T\epsilon_{kB}(p-2j\omega_0)}) \frac{A_y(p)}{B_y(p)} + \\
 &\frac{1}{3} \Delta V_{dc} \frac{1}{p+2j\omega_1} \frac{e^{pT}}{e^{pT} - e^{j(\frac{\pi}{3}-2\omega_1 T)}} \\
 &+ \left. \sum_k (e^{-T\epsilon_{kA}(p+2j\omega_0)} - e^{-T\epsilon_{kB}(p+2j\omega_0)}) \frac{A_y(p)}{B_y(p)} \right\} = \\
 &R_1(e^{pT})Q_1(p) + R_2(e^{pT})Q_2(p) + R_3(e^{pT})Q_3(p)
 \end{aligned} \tag{A1}$$

where the polynomials are as follows:

$$\begin{aligned}
 R_1(e^{pT}) &= \frac{e^{pT}}{e^{pT} - e^{j\frac{\pi}{3}}} \\
 R_2(e^{pT}) &= \frac{e^{pT}}{e^{pT} - e^{j(\frac{\pi}{3}+2\omega_1 T)}} \\
 R_3(e^{pT}) &= \frac{e^{pT}}{e^{pT} - e^{j(\frac{\pi}{3}-2\omega_1 T)}}
 \end{aligned} \tag{A2}$$

$$\begin{aligned}
 Q_1(p) &= \frac{2}{3} V_{dc} \frac{1}{p} \\
 &+ \sum_k (e^{-pT\epsilon_{kA}} - e^{-pT\epsilon_{kB}}) \frac{A_y(p)}{B_y(p)} \\
 Q_2(p) &= \frac{1}{3} \Delta V_{dc} \frac{1}{p-2j\omega_1} \\
 &+ \sum_k (e^{-T\epsilon_{kA}(p-2j\omega_0)} - e^{-T\epsilon_{kB}(p-2j\omega_0)}) \frac{A_y(p)}{B_y(p)} \\
 Q_3(p) &= \frac{1}{3} \Delta V_{dc} \frac{1}{p+2j\omega_1} \\
 &+ \sum_k (e^{-T\epsilon_{kA}(p+2j\omega_0)} - e^{-T\epsilon_{kB}(p+2j\omega_0)}) \frac{A_y(p)}{B_y(p)}
 \end{aligned} \tag{A3}$$

As can be seen from (A1), the Laplace transform of the motor current consists of three terms, each with two multiplicative parts. One ($R(e^{pT})$) is a function of e^{pT} -operator, the other ($Q(p)$) is a function of p -operator. To find original function of (A1) we can use the residual theorem.

But the inverse transform of (A1) can not be carried out in direct way as it contains infinite number of poles given by

$$\begin{aligned}
 e^{pT} - e^{j\frac{\pi}{3}} &= 0, e^{pT} - e^{j(\frac{\pi}{3}+2j\omega_1 T)} = 0, \\
 e^{pT} - e^{j(\frac{\pi}{3}-2j\omega_1 T)} &= 0
 \end{aligned} \tag{A4}$$

From (A1) it may be seen that using superposition each term can be separated into two multiple parts and so we can transform (A1) into the modified Z transform [13]. If doing so, we get in the modified Z-space:

$$\begin{aligned}
 I_y(z, \epsilon) &= R_1(z) \cdot Z_m\{Q_1(p)\} + R_2(z) \cdot Z_m\{Q_2(p)\} + \\
 &R_3(z) \cdot Z_m\{Q_3(p)\}
 \end{aligned} \tag{A5}$$

with $Z_m\{\}$ denoting the modified Z transform operator.

In order to find Z transform of $Q_i(p)$ we must use the translation theorem in Z transform which holds:

$$Z_m\{e^{-p \cdot a} \cdot F(p)\} = z^{-x} \cdot F(z, \epsilon - a + x) \tag{A6}$$

where parameter x is given by:

$$x = \begin{cases} 1 & \text{for } 0 \leq \epsilon < a \\ 0 & \text{for } a \leq \epsilon < 1 \end{cases} \tag{A7}$$

If we want to express translation for k -the pulse, with the beginning ϵkA and the end ϵkB , (pulse-width $\Delta \epsilon k = \epsilon kB - \epsilon kA$) we can use two parameters, namely M_k and L_k to determine per unit time for prepulse, inside-pulse and postpulse switching times, respectively. M_k is a parameter that defines the beginning of k -the pulse ϵkA , L_k is a parameter that defines the end of the k -the pulse ϵkB . According to (A6) we can write for m_k and n_k , respectively:

$$M_k = \begin{cases} 1 & \text{for } 0 \leq \epsilon < \epsilon kA \\ 0 & \text{for } \epsilon kA \leq \epsilon < 1 \end{cases} \quad L_k = \begin{cases} 1 & \text{for } 0 \leq \epsilon < \epsilon kB \\ 0 & \text{for } \epsilon kB \leq \epsilon < 1 \end{cases} \tag{A8}$$

By means of these two parameters we can express per unit time for the three intervals:

- a) $0 < \epsilon \leq \epsilon_{kA}$ prepulse per unit time. $M_k=1, L_k=1$

- b) $\epsilon_{kAQ} < \epsilon \leq \epsilon_{kB}$ inside pulse per unit time $M_k=0, L_k=1$
 - c) $\epsilon_{kB} < \epsilon \leq 1$ postpulse per unit time $M_k=0, L_k=0$
- (A9)

Thus, in a period nT , for per unit time $0 < \epsilon \leq 1$, we obtain from (A9) two parameters M_k and L_k , that will be used for solution of (A3) in the modified Z transform.

Using parameters M_k, L_k and Heaviside theorem (12), we can express the first part of (A1) with help of (A9) in the modified Z-space as follows:

$$I^1_{yS}(n, \epsilon) = \frac{2V_{dc}}{3} \frac{z}{z - e^{j\frac{\pi}{3}}} \sum_k \left\{ \frac{A_y(0) e^{\frac{j\pi\alpha_k}{3}}}{B_y(0)} \frac{z}{z-1} (z^{-M_k} - z^{-L_k}) + \sum_{s=1}^2 \frac{A_y(p_s)}{p_s B_y'(p_s)} e^{\frac{j\pi\alpha_k}{3}} \frac{z e^{p_s T \epsilon}}{z - e^{p_s T}} \right\} \left[\begin{array}{l} z^{-M_k} e^{p_s T (M_k - \epsilon_{kA})} - z^{-L_k} e^{p_s T (L_k - \epsilon_{kB})} \end{array} \right] \quad (A10)$$

Equation (A10) has simple poles $e^{j\pi/3}, 1, p_s T$. The inverse Z transform of (A10) can be found using an integral

$$I^1(n, \epsilon) = \frac{1}{2\pi j} \oint I^1(z, \epsilon) z^{n-1} dz \quad (A11)$$

An integral (A11) may be solved by means of the residual theorem. As our attention is the steady-state components we get for $n \rightarrow \infty$ the following expression:

$$I^1_{yS} = \sum_k \left\{ \frac{2V_{dc}}{3} e^{j\frac{\pi\alpha_k}{3}} \left[\frac{A_y(0) (e^{-j\frac{\pi}{3} M_k} - e^{-j\frac{\pi}{3} L_k})}{B_y(0) (e^{j\frac{\pi}{3}} - 1)} + \frac{A_y(p_s)}{\sum_{s=1}^2 p_s B_y'(p_s) (e^{j\frac{\pi}{3}} - e^{p_s T})} \right] \left[\begin{array}{l} e^{-j\frac{\pi}{3} M_k + p_s T (M_k - \epsilon_{kA})} - e^{-j\frac{\pi}{3} L_k + p_s T (L_k - \epsilon_{kB})} \end{array} \right] \right\} = I^1_{yS}(0) + I^1_{yS}(p_s) \quad (A12)$$

Equation (A12) is the time dependency of the first part of the current space vector in the stator co-ordinate system. By the same way and using the theorem for multiplication by an exponential function (13) we can

derive overall solution given in (14). The corresponding coefficients are given in (A13) and (A14).

$$I^2_{yS} = \sum_{s=1}^2 \frac{\Delta V_{dc}}{3} \frac{A_s(2j\omega_1)}{B_s(2j\omega_1)} \sum_k \left[\frac{(e^{-j\frac{\pi}{3} M_k} - e^{-j\frac{\pi}{3} L_k})}{(e^{j\frac{\pi}{3}} - 1)} e^{j\frac{\pi}{3} \alpha_k} \right] + \sum_{s=1}^2 \frac{\Delta V_{dc}}{3} \frac{A_s(p_s)}{(p_s - 2j\omega_1) B'_s(p_s)} \left[\begin{array}{l} (e^{-j\frac{\pi}{3} M_k - 2j\omega_1 T (M_k - \epsilon_{Ak}) + p_s T (M_k - \epsilon_{Ak})} - e^{-j\frac{\pi}{3} L_k - 2j\omega_1 T (L_k - \epsilon_{Bk}) + p_s T (L_k - \epsilon_{Bk})}) e^{j\frac{\pi}{3} \alpha_k} \\ (e^{j(\frac{\pi}{3} + 2j\omega_1 T)} - e^{p_s T}) \end{array} \right] = (A13)$$

$$I^2_{yS}(2j\omega_1) + I^2_{yS}(p_s - 2j\omega_1)$$

$$I^3_{yS} = \sum_{s=1}^2 \frac{\Delta V_{dc}}{3} \frac{A_s(-2j\omega_1)}{B_s(-2j\omega_1)} \sum_k \left[\frac{(e^{-j\frac{\pi}{3} M_k} - e^{-j\frac{\pi}{3} L_k})}{(e^{j\frac{\pi}{3}} - 1)} e^{j\frac{\pi}{3} \alpha_k} \right] + \sum_{s=1}^2 \frac{\Delta V_{dc}}{3} \frac{A_s(p_s)}{(p_s + 2j\omega_1) B'_s(p_s)} \left[\begin{array}{l} (e^{-j\frac{\pi}{3} M_k + 2j\omega_1 T (M_k - \epsilon_{Ak}) + p_s T (M_k - \epsilon_{Ak})} - e^{-j\frac{\pi}{3} L_k + 2j\omega_1 T (L_k - \epsilon_{Bk}) + p_s T (L_k - \epsilon_{Bk})}) e^{j\frac{\pi}{3} \alpha_k} \\ (e^{j(\frac{\pi}{3} - 2j\omega_1 T)} - e^{p_s T}) \end{array} \right] = (A14)$$

$$I^3_{yS}(-2j\omega_1) + I^3_{yS}(p_s + 2j\omega_1)$$

Provided that an assumption of constant rotor speed is made it can be seen, that the solution (14) is in closed-form. For concrete solution we must substitute into (A10) only parameters of the load $(A(p), B(p))$ and parameters of the inverter $(V_{dc}, \epsilon_{kA}, \epsilon_{kB}, \alpha_k)$

The induction motor used both for the analytical and experimental investigation was rated at 400/230V, 1.5kW, and 1430 rpm. Its per unit parameters are $R_S=0.068, R_R=0.07, L_S=L_R=1.39$, and $L_m=1.382$

Reference:

- [1] DE ABREU, J.P.G., EMANUEL, A.E.: Induction motor thermal aging caused by voltage distortion and unbalance: Loss of useful life and its estimated cost. *IEEE Trans. Ind. Appl.*, vol 38, no 1, pp.12-20, Jan/Feb 2000.
- [2] MORAN, L., ZIOGAS, P.D.Z., JOOS, G.: Design aspects of synchronous PWM rectifier-inverter systems under unbalanced input voltage conditions. *IEEE Trans. Ind. Appl.*, vol 28, no 6, pp.1286-1293, Nov/Dec 1992.
- [3] LEE, L., JAHNS, T. M., LIPO T.A. : Closed-form analysis of adjustable-speed drive performance under input-voltage unbalance and sag conditions. *IEEE Trans. Ind. Appl.*, vol 42, no 3, pp.731-741, May/June 2006
- [4] CROSS, A.M., EVANS, P.D., FORSYTH, A.J.: DC link current in PWM inverters with unbalanced and non-linear loads. *IEE Proc. Electr. Pow. Appl.* Vol.143, No.6, 1999, pp.620-626
- [5] CHOMAT, M., SCHREIER, L.: Control Method for DC-link Voltage Ripple Cancellation in Voltage Source Inverter Under Unbalanced Three-Phase Voltage Supply Conditions. *IEE Proc. Electric Power Appl.* Vol.152, Issue 3, May 2005, pp.494-500.
- [6] BROECK H.W., SKUDELNY H.C.: Analytical Analysis of the Harmonic Effects of a PWM AC Drive. *IEEE Trans. Power Electron.* 1988, (2), pp.216-222.
- [7] BROECK H.W., WYK J.D.: A Comparative Investigation of a Three-Phase Induction Machine Drive with a Component Minimised Voltage-Fed Inverter under Different Control Options. *IEEE Trans. Ind. Appl.* 1984, (2), pp.309-320.
- [8] ANDERSEN, E. C., HAUN, A., Influence of the pulsewidth modulation control method on the performance of frequency inverter induction motor drives," *European Trans.on Electric Power (ETEP)*, vol.3, 1993, pp.151-161
- [9] HOLTZ, J, Identification and compensation of torque ripple in high-precision permanent magnet motor drives," *IEEE Trans. Ind. Electron.*, vol.43, no.2, 1996, pp.309-320
- [10] HOFMAYER, F: Harmonic torque pulsation of induction machines-Analysis and compensation techniques using PWM inverters," *EPE Conference*, Toulouse, France, 2003 pp.247-251
- [11] CHOMAT, M., SCHREIER, L.: Compensation of Unbalanced Three-Phase Voltage Supply in Voltage Source Inverter. *Proc. 28th Annual Conference of the IEEE Industrial Society*, 2002, pp.950-955
- [12] KLIMA J.: Analytical Closed-Form Solution of a Space-Vector Modulated VSI Feeding an Induction Motor Drive. *IEEE Transaction on Energy Conversion*. Vol.17, No2, June 2002.
- [13] KLIMA J.: Mixed p-z Approach for Analytical Analysis of an Induction Motor fed from Space-Vector PWM Voltage Source Inverter. *European Trans.on Electric Power (ETEP)* Vol.12, November/December, 2002.
- [14] KLIMA J.: Mixed p-z approach for time-domain analysis of voltage source inverters with periodic pulse width modulation. *IEEE Trans. on Circuits and Syst-II* vol.51, no.10, 2004, pp.529-536

